

Research Article

Comparative impact of natural crosslinking, plasticization, and hydrophobic additives on the physicochemical properties of rice husk-starch biodegradable straws

Nur Irdina Kamarul Bahrin¹, Rozaini Abdullah^{1,2*}, Ku Syahidah Ku Ismail^{1,3}, and Muhammad Akmal Amir⁴

¹ Faculty of Chemical Engineering & Technology, Universiti Malaysia Perlis, 02600, Arau, Perlis, Malaysia

² Centre of Excellence for Frontier Materials Research, Universiti Malaysia Perlis, No. 64-66, Blok B, Taman Pertiwi Indah, Jalan Kangar - Alor Setar, Kampung Seriab, 01000 Kangar, Perlis, Malaysia

³ Centre of Excellence for Biomass Utilization, Kompleks Pusat Pengajian Jejawi 3, Kawasan Perindustrian Jejawi, Universiti Malaysia Perlis, 02600 Arau, Perlis, Malaysia

⁴ Ada Biotech Sdn Bhd, Lot 5497, Tingkat Mak Mandin 4, Mak Mandin Industrial Estate, 13400 Butterworth, Pulau Pinang, Malaysia

*Corresponding author: rozainiabdullah@unimap.edu.my

Received: 24 September 2025; Revised: 30 March 2026; Accepted: 6 April 2026; Published: 28 April 2026

Abstract

Starch-based biodegradable straws offer a sustainable alternative to petroleum-based plastics, yet their practical application is limited due to poor water resistance and insufficient mechanical strength. In the present study, drinking straws made of corn starch, rice husk, carboxymethyl cellulose, and water were prepared using a twin-screw extrusion process. To systematically evaluate different chemical pathways, candelilla wax, glycerol, and citric acid were introduced separately to investigate the effect of hydrophobic modification, plasticization, and crosslinking under identical processing conditions. The resulting drinking straws underwent comprehensive physicochemical characterization, encompassing water uptake behavior, mechanical flexural performance, FTIR spectroscopy analysis, and thermogravimetric (TGA) profiling, followed by soil burial biodegradation. The candelilla wax formulation exhibited the lowest water absorption ($53.90 \pm 2.99\%$) and the highest flexural strength (16.54 ± 1.86 MPa), whereas the citric acid formulation achieved the lowest strength (9.33 ± 1.38 MPa), indicating increased brittleness. All formulations demonstrated biodegradability, with the control showing a degradation rate of $76.45 \pm 8.27\%$ after 28 days, while the modified formulations showed lower degradation due to limited moisture diffusion. Overall, hydrophobic modification via candelilla wax was the most balanced in performance by improving moisture resistance and mechanical stability while maintaining biodegradability.

Keywords: drinking straw, natural crosslinking, candelilla wax, biodegradable, water resistance

Introduction

The extensive use of synthetic plastics in modern applications is largely due to their durability, versatility, and low production costs, especially in packaging and single-use products [1,2]. However, the persistence of petroleum-based plastics in natural environments has raised serious environmental concerns. As of 2015, the global cumulative amount of plastics produced was approximately 8.3 billion tonnes, with most of the materials ending up as waste due to low recycling capacity [3]. Recycling rates are also low globally, with only about 9% of plastic waste recycled, and the rest is either landfilled, incinerated, or discharged into the environment due to inadequate

waste management systems [4,5]. In addition, large amounts of plastic waste continue to enter marine environments each year, leading to long-term ecological pollution and the production of microplastics [6,7]. These concerns have led to an increased development of biodegradable materials as sustainable alternatives. Starch-based biocomposites have emerged as a prominent sustainable material due to their renewability, cost-effectiveness, and excellent processability via thermoplastic techniques, making them highly suitable for single-use applications such as drinking straws.

Agricultural residues are increasingly used as

reinforcing agents in biodegradable polymer systems. Rice husk is a major lignocellulosic by-product of rice milling, and global production generates substantial quantities each year. Estimates indicate that approximately 148 million tonnes of rice husk are produced globally each year [8,9]. In Malaysia, rice husk is a valuable biomass resource with great potential for utilization. Its composition, which is mainly cellulose, hemicellulose, lignin, and a relatively high silica content, contributes to structural rigidity and makes it suitable as a reinforcing filler in polymer composites [10,11]. When used in a starch matrix, rice husk can improve stiffness and dimensional stability. However, starch-based materials are intrinsically hydrophilic due to numerous hydroxyl groups, leading to poor water resistance and mechanical performance under humid conditions [12,13]. To overcome these limitations, several modification strategies have been investigated. Hydrophobic additives (e.g., natural waxes) reduce moisture sensitivity by forming dispersed hydrophobic domains that limit water diffusion [14]. Plasticizers such as glycerol increase polymer chain mobility by weakening intermolecular hydrogen bonds, thereby improving flexibility and processability [15]. Crosslinking agents, such as citric acid, form covalent ester bonds with starch chains, resulting in a more compact network with enhanced water resistance and mechanical stability [16].

Despite these improvements, most reported studies use these modification strategies independently or require additional pre- or post-extrusion processing steps. Crosslinking is often carried out after extrusion by chemical treatment or retrogradation, which increases processing complexity and production time [17]. Similarly, hydrophobic modification is often accomplished using post-forming coating techniques, such as wax immersion, which add extra manufacturing steps and are difficult to scale up. Similarly, hydrophobic modification is often accomplished using post-forming coating techniques, such as wax immersion, which introduce additional manufacturing steps and are difficult to scale up [18]. Furthermore, the fundamental interactions underlying crosslinking, plasticization, and hydrophobic phase formation in a single starch-based system are not well understood. Additionally, the specific mechanisms by which these modifications influence polymer chain mobility, structural integrity, and the moisture diffusion pathway under consistent extrusion parameters remain poorly understood. Consequently, the relative contributions of crosslinking, plasticization, and hydrophobic modification to the

functional performance of starch-based straws require further investigation under controlled formulation and processing conditions.

In this study, citric acid, glycerol, and candelilla wax were directly incorporated into the rice husk-starch formulation before extrusion, allowing simultaneous interaction with the polymer matrix during extrusion without additional processing steps. The objective is to assess the impact of these additives on the mechanical, physicochemical, and thermal characteristics of biodegradable straws. It is hypothesized that citric acid would increase network stiffness and water resistance via ester-based covalent crosslinking, thereby reducing polymer chain mobility and increasing structural integrity. Glycerol is expected to exert a plasticizing effect by breaking intermolecular hydrogen bonds, increasing free volume and segmental mobility in the starch matrix, and enhancing flexibility. In contrast, candelilla wax is expected to limit water intake by forming dispersed hydrophobic domains that restrict the diffusion pathways for moisture in the heterogeneous composite matrix. This comparative approach enables systematic evaluation of structure-property relationships in additive-matrix interactions and offers a simplified, scalable strategy for biodegradable straw production.

Materials and Methods

Materials

Corn starch, carboxymethyl cellulose (CMC), citric acid, glycerol, and candelilla wax were purchased from a local food-grade supplier in Perlis, Malaysia, and used as received. Rice husk was acquired from a local rice milling plant in Perlis, Malaysia. The soil for biodegradation experiments consisted of palm sludge, black soil, commercial biochar, and probiotic additives, obtained from a local nursery in Perlis, Malaysia.

Preparation of biodegradable drinking straws

Biodegradable drinking straws were prepared using a starch-based formulation expressed in parts per hundred resin (phr), where corn starch was defined as the reference component (100 phr). Rice husk powder and carboxymethyl cellulose (CMC) were incorporated at 7.86 phr and 2.14 phr, respectively, while distilled water was added at 32.86 phr to facilitate gelatinization and extrusion processability. Candelilla wax, glycerol, and citric acid were separately incorporated at 2.14 phr by partially replacing starch. The formulation codes are summarized in **Table 1**.

Table 1. Formulation codes and composition (phr) of biodegradable straws

Formulation Code	Starch (phr)	Rice Husk (phr)	CMC (phr)	Water (phr)	Additive (phr)	Additive Type
FS-CTRL	100	7.86	2.14	32.86	-	Control (No Additive)
FS-CW	100	7.86	2.14	32.86	2.14	Candellila Wax
FS-GLY	100	7.86	2.14	32.86	2.14	Glycerol
FS-CA	100	7.86	2.14	32.86	2.14	Citric Acid

Notes: phr = parts per hundred resin, where corn starch is defined as 100 phr.

All components were premixed using a laboratory mixer to ensure uniform distribution, followed by the gradual addition of water to obtain a homogeneous mixture suitable for extrusion. The mixture was processed in a pilot-scale twin-screw extruder with a tubular die. The extrusion parameters were adapted from previously reported starch-based drinking straw production [17]. The barrel temperature profile was set at 50 °C, 70 °C, and 105 °C, with a screw speed of 120 rpm and a feed rate of 7 kg/h. The die dimensions were 4.1 mm (inner diameter) and 7.5 mm (outer diameter), which yielded straws with an average wall thickness of 1.7 mm. The residence time was estimated to be 45-90 seconds. Extruded tubes were cut into 200 mm lengths, dried at 50 °C for 4 hours until constant weight, and stored in a desiccator prior to characterization.

Water absorption test

The water absorption behavior was evaluated by immersion at 4 °C and 25 °C. Samples were oven-dried at 70 °C for 24 hours to obtain a constant initial weight (W_i) and cut into 60 mm segments. Samples were immersed in 100 mL of distilled water at the respective temperatures, and weight was recorded at 15, 30, 60, 120, and 240 minutes [19]. At each interval, samples were removed, blotted, and weighed (W_f). Measurements were performed in five replicates. Water absorption (W_A , %) was calculated according to the following equation, Eq. (1):

$$W_A(\%) = \frac{W_f - W_i}{W_i} \times 100\% \quad (\text{Eq. 1})$$

Flexural strength test

The flexural strength was determined using a three-point bending test based on ISO 178:2019, with modifications for hollow cylindrical specimens. Before testing, samples were conditioned at 23 ± 2 °C and $50 \pm 5\%$ relative humidity for 24 hours and cut into 80 mm segments. The test was conducted using a texture analyzer (Stable Micro Systems, UK) with a

support span of 52 mm and a crosshead speed of 0.5 mm/s, as reported by Zhang et al. [19]. The span length was selected to provide stable loading of the hollow specimens. The maximum load at fracture (F) was recorded and used to calculate the flexural strength (σ_f) based on the bending stress equation for hollow circular beams, as shown in Eq. (2):

$$\sigma_f(\text{MPa}) = \frac{8FLD_o}{\pi(D_o^4 - D_i^4)} \quad (\text{Eq. 2})$$

where F is the maximum load, L is the span length, D_o is the outer diameter, and D_i is the inner diameter. All measurements were carried out in five replicates.

Functional group analysis

Functional group analysis was performed by Fourier transform infrared (FTIR) spectroscopy (PerkinElmer, USA). Powdered samples were mixed with anhydrous potassium bromide (KBr) at a 1:10 (w/w) ratio and pressed into pellets. Spectra were captured over 450-4000 cm^{-1} at 4 cm^{-1} resolution with 16 scans [20].

Thermal stability analysis

Thermogravimetric analysis was conducted using a thermogravimetric analyzer (TGA) (Perkin Elmer, USA). Approximately 10 mg of sample was placed in an aluminum sample pan and heated from 30 °C to 600 °C at 20 °C/min under nitrogen flow (20 mL/min) [17]. Weight loss was measured as a function of temperature.

Soil burial degradation test

Biodegradability was assessed using a soil burial method under natural conditions. Samples (60 mm) were oven-dried at 70 °C for 24 hours to obtain the initial weight (W_i) and buried at a depth of 40 mm in prepared soil. Soil pH ranged from 5.0 to 5.8, and moisture content was maintained at 25-35%. Samples were retrieved at 0, 7, 14, 21, 28, 35, and 42 days, briefly rinsed with distilled water, and oven-dried at 70 °C for 24 hours to obtain the final weight (W_f) [21].

Measurements were performed in five replicates. Weight loss (W_L , %) was calculated using Eq. (3):

$$W_L(\%) = \frac{w_i - w_f}{w_i} \times 100\% \quad (3)$$

Statistical analysis

All experimental results are expressed as mean \pm standard deviation (SD). Statistical analysis was conducted using Minitab 22.3.1 (Minitab Inc., USA). Significant differences among samples were analyzed using one-way analysis of variance (ANOVA) followed by Tukey's post-hoc test at a significance level of $p < 0.05$.

Results and Discussion

Water absorption behavior

Water absorption behavior is a key indicator of the durability of starch-based drinking straws, as moisture uptake can promote swelling of the polymer matrix and gradually weaken structural integrity during beverage exposure. The absorption profiles of the drinking straws were therefore evaluated at 4 °C and 25 °C, representing refrigerated and ambient beverage temperatures. The absorption profiles illustrated in **Figure 1** indicate that all formulations exhibited a similar pattern, characterized by a rapid initial uptake during the first 60 minutes, followed by a slower increase towards equilibrium between 120 and 240 minutes. Such behavior is typical of hydrophilic starch-based polymers. The initial stage is associated with the adsorption of water molecules onto hydroxyl-rich starch surfaces and capillary penetration into microvoids within the polymer structure. As immersion continues, the diffusion within the polymer network becomes dominant. It is accompanied by

gradual swelling until equilibrium is established between absorbed moisture and the elastic resistance of the polymer structure. Comparable diffusion-controlled moisture-uptake behavior has been reported for starch-based biopolymer materials in aqueous environments [22-25].

Temperature clearly influenced the equilibrium absorption behavior of the straws. For example, at 25 °C, water absorption values after 240 minutes ranged from $53.90 \pm 2.99\%$ to $62.46 \pm 3.01\%$, with the control formulation showing $55.80 \pm 0.42\%$, whereas lower values between $48.68 \pm 2.51\%$ and $55.55 \pm 2.46\%$ were obtained at 4 °C, where the control sample exhibited $50.71 \pm 1.89\%$. Statistical evaluation using one-way ANOVA indicated that the additive composition significantly influenced absorption at 25 °C ($F = 4.36$, $p = 0.043$). Post hoc Tukey analysis revealed that the glycerol formulation, FS-GLY, had significantly higher water absorption than the candelilla wax formulation, FS-CW ($p < 0.05$). In contrast, the citric acid formulation, FS-CA, and the control formulation, FS-CTRL, were not significantly different from either group. In contrast, no statistically significant difference among formulations was observed at 4 °C ($F = 3.70$, $p = 0.062$). The higher absorption observed at elevated temperatures is probably due to increased molecular kinetic energy, which enhances polymer chain mobility and facilitates the diffusion of water molecules within the matrix. On the other hand, reduced molecular motion at lower temperatures limits polymer relaxation and swelling of the hydrophilic starch phase. Similar temperature-dependent moisture interactions have been reported in thermoplastic starch materials where polymer mobility controls water diffusion behavior [26].

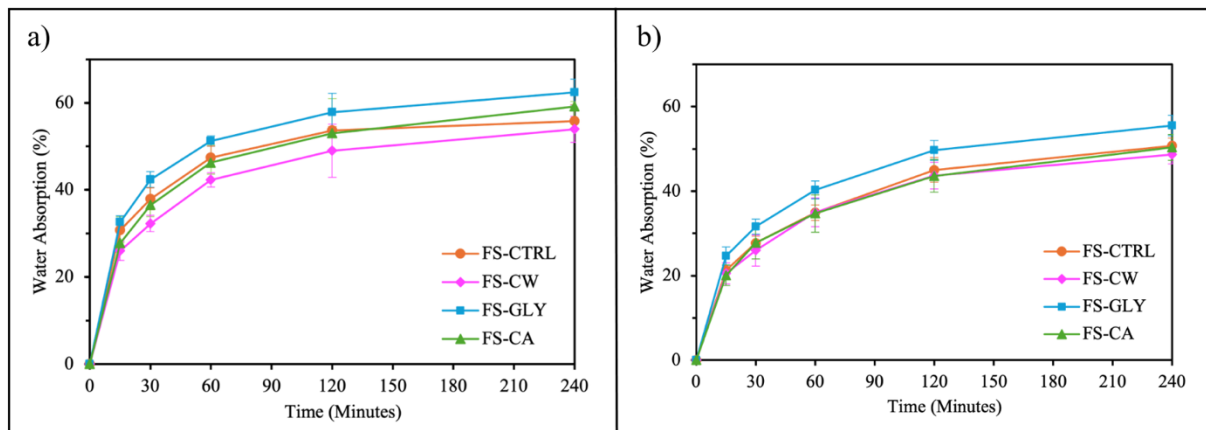


Figure 1. Water absorption of biodegradable straw formulations under different temperature conditions: a) 25 °C and b) 4 °C. **Notes:** Values are expressed as mean \pm SD ($n = 5$).

Differences between formulations are primarily associated with the structural role of the additives within the composite matrix. FS-CTRL represents the baseline hydrophilic starch system, where abundant hydroxyl groups facilitate water sorption through hydrogen bonding. FS-CW consistently exhibited the lowest absorption values, reaching $53.90 \pm 2.99\%$ at $25\text{ }^{\circ}\text{C}$ and $48.68 \pm 2.51\%$ at $4\text{ }^{\circ}\text{C}$. This behavior is likely attributed to the formation of hydrophobic wax domains within the starch matrix, which reduce the accessibility of hydrophilic sorption sites and increase the tortuosity of diffusion pathways, thereby limiting water transport. Comparable moisture-barrier effects have been documented in wax-modified starch composites, where wax incorporation improves dimensional stability during water exposure [18,27]. In contrast, FS-GLY exhibited the highest water absorption, reaching $62.46 \pm 3.01\%$ at $25\text{ }^{\circ}\text{C}$ and $55.55 \pm 2.46\%$ at $4\text{ }^{\circ}\text{C}$. This behavior is associated with plasticization, in which glycerol increases free volume and enhances polymer chain mobility within the starch network, thereby facilitating the diffusion of water molecules through the matrix. This trend is consistent with observations reported for glycerol-plasticized thermoplastic starch systems [28–30].

FS-CA exhibited intermediate water absorption values of $59.14 \pm 4.59\%$ at $25\text{ }^{\circ}\text{C}$ and $50.34 \pm 3.50\%$ at $4\text{ }^{\circ}\text{C}$. Citric acid reacts with hydroxyl groups of starch molecules to form ester linkages, introducing covalent crosslinks within the polymer network. This esterification decreases the number of available hydrophilic sorption sites and restricts polymer chain expansion, which would be expected to limit water uptake. However, the present results suggest that the degree of crosslinking achieved only moderately attenuated moisture diffusion through the composite matrix. This effect is likely influenced by increased polymer chain mobility at higher temperatures, which can partially offset the restrictive effect of crosslinking and allow continued water diffusion. Such behavior has been observed in citric-acid-modified starch systems, where the effectiveness of crosslinking depends strongly on crosslink density and processing conditions [31]. Overall, the equilibrium absorption values obtained in this study (48–62%) fall within the range commonly reported for starch-based biodegradable drinking straws, typically

around 45–80% depending on formulation and testing conditions [21]. From a functional perspective, formulations with lower moisture uptake, particularly the wax-based system, are expected to retain structural integrity for extended periods during beverage exposure.

Flexural strength performance

Flexural strength represents the maximum bending stress before fracture and reflects the mechanical stability of the drinking straws. The measured values ranged from 9.33 to 16.54 MPa (**Table 2**), indicating variability among the formulations. The candelilla wax formulation, FS-CW, exhibited the highest mean value of 16.54 ± 1.86 MPa, whereas the citric acid formulation, FS-CA, showed the lowest value of 9.33 ± 1.38 MPa. The glycerol formulation, FS-GLY, and the control formulation, FS-CTRL, recorded intermediate values of 15.40 ± 2.09 MPa and 13.78 ± 0.71 MPa, respectively.

This behavior is owing to the presence of dispersed hydrophobic wax domains in FS-CW, which decrease internal voids and increase matrix density, thereby improving stress transfer between the starch phase and rice husk fibers during bending. The starch matrix likely serves as the primary load-bearing interface, maintaining interfacial adhesion despite the low polarity of the wax. Comparable densification-driven reinforcement has been reported in starch-fiber composites containing lipid additives [32,33]. This interpretation is consistent with the lower water absorption, suggesting a more compact and less permeable structure.

In contrast, the behavior of FS-GLY is related to plasticization, in which glycerol disrupts intermolecular hydrogen bonding and increases free volume within the starch network. The resulting increase in chain mobility reduces brittleness and facilitates stress redistribution, thus delaying crack propagation during bending. Equivalent behavior has been reported in thermoplastic starch systems where plasticization enhances flexibility while maintaining moderate strength [28–30]. The higher water absorption observed for FS-GLY supports this interpretation, as increased free volume promotes moisture diffusion [15].

Table 2. Flexural strength of biodegradable drinking straws

Formulation Code	Flexural Strength (MPa)
FS-CTRL	13.78 ± 0.71^a
FS-CW	16.54 ± 1.86^a
FS-GLY	15.40 ± 2.09^a
FS-CA	9.33 ± 1.38^b

Notes: Values are presented as mean \pm standard deviation ($n = 5$). ‘a’ means not statistically significant ($p > 0.05$), while ‘b’ means significantly different ($p < 0.05$).

FS-CA showed the lowest flexural strength due to crosslinking effects. Citric acid forms ester crosslinks with starch chains, increasing network rigidity, as supported by FTIR analysis [34,35]. However, excessive crosslink density limits chain mobility and promotes brittle fracture under bending stress. Similar trends have been reported in crosslinked starch systems where increased stiffness is accompanied by reduced mechanical durability [36]. Statistical analysis further confirmed these observations, where one-way ANOVA displayed a significant effect of formulation ($F = 19.54$, $p < 0.001$). Tukey's analysis (post hoc test) confirmed that FS-CA was significantly different from the other samples ($p < 0.05$), while FS-CW, FS-GLY, and FS-CTRL showed no significant differences. Despite this limitation, the values obtained for FS-CTRL, FS-GLY, and FS-CW (13.78 ± 0.71 , 15.40 ± 2.09 , and 16.54 ± 1.86 MPa) remain within the typical range for biodegradable starch straws (12–23 MPa) [19].

Functional group analysis

FTIR spectra (**Figure 2**) denote that all formulations preserve a polysaccharide-dominated structure. A broad absorption band at approximately 3400 cm^{-1} corresponds to O-H stretching of hydroxyl groups, reflecting extensive intra- and intermolecular hydrogen bonding within the matrix [37]. These hydroxyl-rich structures support strong interactions with water molecules, consistent with the moisture-uptake behavior observed during immersion testing [38,39]. Variations in the O-H region reflect differences in additive-polymer interactions. The glycerol formulation, FS-GLY, displayed a broader absorption band, which indicates redistribution of hydrogen bonding due to glycerol incorporation. Glycerol molecules interact with starch hydroxyl groups and modify the native intermolecular association within the polysaccharide network. This interaction increases the availability of hydrophilic sites and is consistent with the higher water absorption observed [40,41]. In contrast, the candelilla wax formulation, FS-CW, showed no new functional groups, confirming that candelilla wax does not chemically alter the matrix. Instead, wax forms a dispersed hydrophobic phase that reduces accessibility of hydroxyl groups and limits moisture transport, which corresponds with the lower water absorption measured [14,42].

A weak absorption band near 1725 cm^{-1} was observed in the citric acid formulation, FS-CA, and is ascribed to carbonyl (C=O) vibrations potentially related to

ester groups or residual carboxylic functionalities derived from citric acid. However, the low intensity of this band indicates that esterification is limited, and FTIR analysis alone does not confirm significant covalent crosslinking within the polymer network [43,44]. This observation is consistent with the lower flexural strength measured for FS-CA, suggesting that chemical modification of the matrix is minimal compared to the physical effects observed in the other formulations.

Thermal analysis

Mass loss around $150\text{ }^{\circ}\text{C}$ and $300\text{ }^{\circ}\text{C}$ (**Figure 3**) reflects the onset of polysaccharide degradation, followed by a major decomposition stage at $300\text{--}350\text{ }^{\circ}\text{C}$ related to depolymerization of starch and degradation of hemicellulosic and cellulose components from the rice husk reinforcement [46,47]. Although identical degradation stages are observed across all formulations, variations in the initial region suggest differences in moisture-matrix interactions. The glycerol formulation, FS-GLY, exhibits lower apparent mass loss at low temperatures, which is attributed to strongly hydrogen-bonded moisture within the glycerol-starch network. Glycerol hydroxyl groups interact with starch chains, modifying intermolecular associations and delaying the release of bound water. In contrast, the control formulation, FS-CTRL, exhibited greater early mass loss, indicating a larger fraction of weakly associated moisture, while the candelilla wax, FS-CW, and the citric acid formulation, FS-CA, displayed intermediate behavior.

At higher temperatures ($350\text{--}600\text{ }^{\circ}\text{C}$), the degradation rate decreases, corresponding to the decomposition of carbonaceous residues [45,46]. FS-GLY and FS-CA have higher residual masses than FS-CTRL and FS-CW, indicating altered carbonization behavior due to additive incorporation. In glycerol systems, thermal dehydration and rearrangement of plasticized polysaccharides promote the formation of stable carbonaceous structures. In FS-CA, limited ester linkage formation alters the degradation pathway and contributes to increased char yield. Conversely, FS-CW exhibited a minimal effect on the chemical degradation pathway, as the wax phase primarily acts as a physical barrier. These trends are consistent with previous observations, where glycerol increased moisture affinity, wax improved structural compactness, and citric acid introduced limited structural modification.

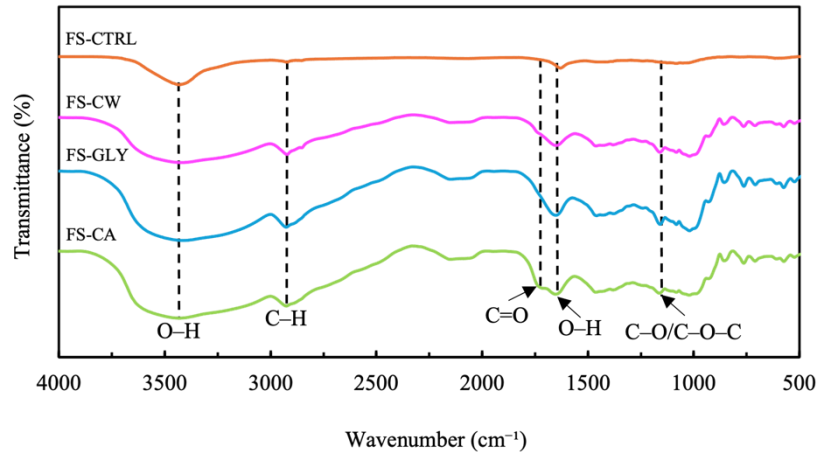


Figure 2. Functional group analysis of biodegradable straw formulations

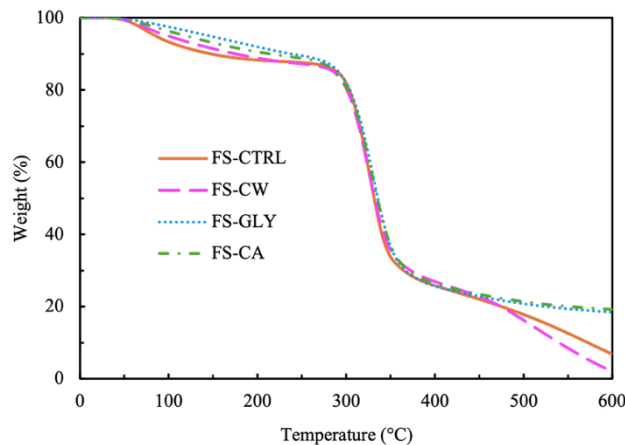


Figure 3. Thermal analysis of biodegradable straw formulations

Soil burial degradation behavior

The soil burial degradation behavior demonstrates the environmental stability of the drinking straw matrix under soil microbial conditions. Starch-based materials generally undergo biodegradation via enzymatic hydrolysis, in which microorganisms metabolize polysaccharides into soluble sugars, which are subsequently mineralized to carbon dioxide and water [48]. Consistent with this mechanism, all formulations exhibited progressive mass loss throughout the burial period (**Figure 4**), indicating continuous microbial utilization of the starch component. Statistical evaluation indicated that formulation composition significantly affected degradation performance ($F = 22.12$, $p < 0.05$). After 28 days, the highest degradation rate of $76.45 \pm 8.27\%$ was observed in the control formulation, FS-CTRL, while the lowest degradation rate of $43.36 \pm 3.54\%$ was observed in the wax formulation, FS-CW. Intermediate degradation rates were observed for the glycerol formulation, FS-GLY, and the citric acid

formulation, FS-CA, with weight loss values of $55.32 \pm 3.92\%$ and $56.15 \pm 2.45\%$, respectively. Tukey's post hoc analysis confirmed that FS-CTRL had significantly greater degradation than the other formulations ($p < 0.05$), and no statistically significant differences were observed among FS-CW, FS-GLY, and FS-CA ($p > 0.05$).

The degradation pattern is consistent with the structural characteristics determined by water absorption, flexural strength, FTIR, and thermal analyses. The reduced degradation rate observed for FS-CW is attributed to the incorporation of candelilla wax, which introduces hydrophobic domains into the composite structure. These nonpolar regions restrict moisture diffusion by increasing the tortuosity of transport pathways and limiting exposure of hydroxyl-rich starch regions to water molecules [49,50]. Reduced moisture penetration delays swelling of the polysaccharide matrix, which is required for microbial colonization and enzymatic hydrolysis. Similar

densification effects have been reported in starch-based composites, where dispersed phases produce a more compact structure with reduced permeability [51]. This structural compactness aligns with the previously observed low water absorption and high flexural strength of FS-CW, indicating that improved internal cohesion confers greater resistance to moisture-induced degradation and microbial infiltration.

On the other hand, the higher degradation observed for FS-GLY is associated with plasticization of the starch matrix. Plasticizers increase the mobility of polymer chains and expand the amorphous regions of the network, thereby facilitating moisture diffusion through the material [52,53]. Increased water uptake promotes swelling of the starch phase and creates favourable conditions for microbial activity. Previous studies on glycerol-plasticized starch systems have similarly reported accelerated biodegradation under soil or compost conditions, due to increased moisture absorption, greater structural flexibility, and enhanced microbial accessibility [53,54]. Consequently, the intermediate degradation behavior of FS-GLY is consistent with the moisture-sensitive nature of plasticized starch composites.

The degradation behavior of FS-CA can be explained by limited esterification within the starch matrix. FTIR analysis showed a weak carbonyl absorption associated with ester linkages formed between the citric acid and the hydroxyl groups of the starch, suggesting partial crosslinking within the polymer network [55,56]. These covalent interactions reduce the availability of free hydroxyl sites and limit initial moisture penetration, thereby delaying hydrolytic degradation at the early stage of soil exposure. However, the relatively low crosslink density allows gradual diffusion of water molecules into the matrix,

enabling microbial enzymes to access unmodified polysaccharide regions over time. This transition accounts for the intermediate degradation profile observed for FS-CA. It should be noted that biodegradation in this study was evaluated solely through mass-loss measurements, and morphological methods, such as scanning electron microscopy, were not employed to directly observe surface erosion or microbial colonization. Thus, the degradation mechanisms are inferred from the physicochemical behavior rather than from direct visualization of the structure.

Conclusion

The effect of crosslinking, plasticization, and hydrophobic modification on rice husk-starch biodegradable straws was systematically evaluated under pilot-scale extrusion conditions. Under identical processing conditions, candelilla wax achieved the lowest water absorption (53.90%) and highest flexural strength (16.54 MPa), while glycerol maintained comparable flexural performance (15.40 MPa) with the highest thermal residue. In comparison, citric acid resulted in intermediate moisture uptake (59.14%) but the lowest mechanical strength (9.33 MPa). These findings directly resolve the previously unclear relative contributions of hydrophobic modification, plasticization, and crosslinking within a single extrusion-based system without additional pre- or post-treatment steps. Candelilla wax was established as the most effective modifier, offering superior moisture resistance and mechanical reinforcement by the formation of hydrophobic domains that restrict water diffusion and enhance structural compactness. Glycerol showed balanced mechanical performance and thermal stability by increasing polymer chain mobility, although at the expense of higher moisture uptake.

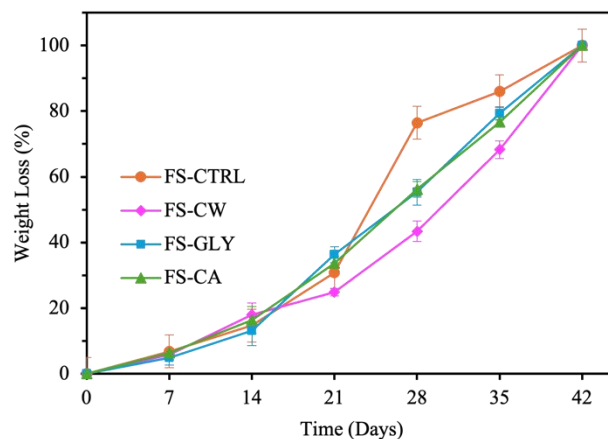


Figure 4. Soil burial degradation of biodegradable straw formulations. *Notes:* Values are expressed as mean \pm SD (n = 3).

In comparison, citric acid demonstrated limited effectiveness in isolation, as insufficient esterification resulted in reduced mechanical strength and increased brittleness. Combined FTIR and TGA analyses revealed that to determine that the predominance of polysaccharide interactions and moisture-dependent thermal behavior controlled the flexural performance and water absorption properties. Biodegradability was validated for all formulations, with degradation reaching 76.45% after 28 days, confirming environmental compatibility and highlighting the barrier effect of the hydrophobic modification. These findings provided clear structure-property relationships and the importance of additive selection in optimizing functional performance. Future work should prioritize synergistic combinations of crosslinking and plasticization strategies, alongside morphological characterization, to further improve the durability and industrial scalability of biodegradable straw systems.

Acknowledgements

We acknowledge the financial support provided by Universiti Malaysia Perlis (UniMAP) and ADA Biotech Sdn. Bhd. through the UniMAP–Private Matching Fund (UniPRIMA), Grant Nos. 9002-00163, 9030-00007, and 9001-00776. Their support was essential for the successful completion of this study.

References

- Roy, P., Ashton, L., Wang, T., Corradini, M. G., Fraser, E. D. G., Thimmanagari, M., Tiessan, M., Bali, A., Saharan, K. M., Mohanty, A. K., and Misra, M. (2021). Evolution of drinking straws and their environmental, economic and societal implications. *Journal of Cleaner Production*, 316, 128234.
- Ni, H., Li, H., Hou, W., Chen, J., Miao, S., Wang, Y., and Li, H. (2024). From sea to sea: Edible, hydrostable, and degradable straws based on seaweed-derived insoluble cellulose fibers and soluble polysaccharides. *Carbohydrate Polymers*, 334, 122038.
- Geyer, R., Jambeck, J. R., and Law, K. L. (2017). Production, use, and fate of all plastics ever made. *Science Advances*, 3(7), e1700782.
- Mazhandu, Z., Muzenda, E., Mamvura, T., Belaid, M., and Nhubu, T. (2020). Integrated and consolidated review of plastic waste management and bio-based biodegradable plastics: Challenges and opportunities. *Sustainability*, 12(20), 8360.
- OECD. (2022). Global plastics outlook: Economic drivers, environmental impacts and policy options. OECD Publishing.
- Ritchie, H. (2023). How much plastic waste ends up in the ocean? Our World in Data. <https://archive.ourworldindata.org/20251125-173858/how-much-plastic-waste-ends-up-in-the-ocean.html>
- Zhang, K., Hamidian, A. H., Tubić, A., Zhang, Y., Fang, J. K. H., Wu, C., and Lam, P. K. S. (2021). Understanding plastic degradation and microplastic formation in the environment: A review. *Environmental Pollution*, 274, 116554.
- Gao, Y., Guo, X., Liu, Y., Fang, Z., Zhang, M., Zhang, R., You, L., Li, T., and Liu, R. H. (2018). A full utilization of rice husk to evaluate phytochemical bioactivities and prepare cellulose nanocrystals. *Science Report*, 8(1), 10482.
- Chen, H., Wang, W., Martin, J. C., Oliphant, A. J., Doerr, P. A., Xu, J. F., DeBorn, K. M., Chen, C., & Sun, L. (2012). Extraction of lignocellulose and synthesis of porous silica nanoparticles from rice husks. *ACS Sustainability Chemical Engineering*, 1(2), 254–259.
- Nguyen, N. T., Tran, N. T., Phan, T. P., Nguyen, A. T., Nguyen, M. X. T., Nguyen, N. N., Ko, Y. H., Nguyen, D. H., Van, T. T. T., & Hoang, D. (2022). Extraction of lignocelluloses and silica from rice husk using a single biorefinery process. *Journal Industrial and Engineering Chemistry*, 108, 150–158.
- Dorairaj, D., & Govender, N. (2023). Rice and paddy industry in Malaysia: Governance and policies. *Frontier Sustainability Food System*, 7, 1093605.
- Johar, N., & Ahmad, I. (2012). Properties of starch biocomposite films reinforced by cellulose nanocrystals. *BioResources*, 7(4), 5469–5477.
- Vieira, E. F., Amaral, T., Domingues, V. F., & Delerue-Matos, C. (2026). Hydrophobicity strategies of starch-based films. *Polymers*, 18(4), 490.
- Alexander, I., Sodri, A., & Mizuno, K. (2023). Effect of natural waxes on hydrophobic properties. *Journal Environmental Science Sustainability Development*, 6(1), 86–101.
- Tarique, J., Sapuan, S. M., & Khalina, A. (2021). Effect of glycerol plasticizer loading. *Science Report*, 11(1), 1–14.
- Wu, H., Lei, Y., Lu, J., Zhu, R., Xiao, D., Jiao, C., Xia, R., Zhang, Z., Shen, G., Liu, Y., Li, S., & Li, M. (2019). Citric acid crosslinking on starch/chitosan films. *Food Hydrocolloids*, 97, 105208.
- He, X., Zhao, S., Zhang, Z., Dai, L., Qin, Y., Ji, N., Xiong, L., Shi, R., & Sun, Q. (2023). Strategy for starch-based straws. *International Journal Biology Macromolecules*, 227, 1089–1097.
- Choeybudit, W., Karbowski, T., Lagorce, A., Ngiwngam, K., Auras, R., Rachtanapun, P.,

- Noiwan, D., & Tongdeesontorn, W. (2024). Eco-friendly straws using soy protein isolate. *Polymers*, 16(13), 1887.
19. Zhang, J., Li, X., Wang, K., Zhu, Y., Guo, L., Cui, B., & Lu, L. (2024). Oil additives on starch straws. *Carbohydrate Polymers*, 334, 122027.
 20. Wang, K., Zou, F., Tao, H., Gao, W., Guo, L., Cui, B., Yuan, C., Liu, P., Lu, L., & Wu, Z. (2023). Cooling temperatures on starch straws. *Carbohydrate Polymers*, 305, 120534.
 21. Wei, X., Tang, J., Tao, H., Gao, W., Guo, L., Cui, B., Liu, P., Lu, L., Wu, Z., Fang, Y., Zhao, M., Yang, N., & Huang, Q. (2022). Cellulose-reinforced starch straws. *Industrial Crops Products*, 189, 115881.
 22. Musa, B. H., & Hameed, N. J. (2021). A study of the effect of starch content on the water absorption of PVA/starch blends. *Engineering and Technology Journal*, 39(1B), 150–158.
 23. Yusuf, Y., Irfandy, F., & Istiani, A. (2022). Mathematical model of water absorption in arrowroot starch-chitosan based bioplastic. *Eksergi*, 19(1), 35.
 24. Ahmad, Z., Razak, N. H. A., Roslan, N. S. M., & Mosman, N. (2014). Evaluation of kenaf fibres reinforced starch based biocomposite film through water absorption and biodegradation properties. *Journal of Engineering Science*, 10, 31.
 25. Ortega-Toro, R., Gonzalez-Cuello, R., & Cortes-Rodriguez, M. (2018). Starch- and PLA-based biocomposites: interactions with water. *Contemporary Engineering Sciences*, 11(40), 1983–1989.
 26. Leroy, L., Stoclet, G., Lefebvre, J.-M., & Gaucher, V. (2022). Mechanical behavior of thermoplastic starch: Rationale for the temperature-relative humidity equivalence. *Polymers*, 14(13), 2531.
 27. Gomes, Á. V. R., Leite, R. H. de L., Silva Júnior, M. Q. da, Santos, F. K. G. dos, & Aroucha, E. M. M. (2019). Influence of composition on mechanical properties of cassava starch, sisal fiber and carnauba wax biocomposites. *Materials Research*, 22, 0887.
 28. Hazrati, K. Z., Sapuan, S. M., Zuhri, M. Y. M., & Jumaidin, R. (2021). Effect of plasticizers on physical, thermal, and tensile properties of thermoplastic films based on *Dioscorea hispida* starch. *International Journal of Biological Macromolecules*, 185, 219–228.
 29. Esmacili, M., Pircheraghi, G., & Bagheri, R. (2017). Optimizing the mechanical and physical properties of thermoplastic starch via tuning the molecular microstructure through coplasticization by sorbitol and glycerol. *Polymer International*, 66(6), 809–819.
 30. Chantawee, K., & Riyajan, S.-A. (2018). Effect of glycerol on the physical properties of carboxylated styrene-butadiene rubber/cassava starch blend films. *Journal of Polymers and the Environment*, 27(1), 50–60.
 31. Gerezgiher, A. G., & Szabó, T. (2022). Crosslinking of starch using citric acid. *Journal of Physics: Conference Series*, 2315(1), 012036.
 32. Arshad, Z., Jahan, Z., Miran, W., Alshareef, R. S., & Niazi, M. B. K. (2026). Innovative utilization of agricultural byproducts: development and analysis of eco-friendly packaging materials from rice husk and wheat straw. *Polymer Bulletin*, 83(5), 224.
 33. Gomes, Á. V. R., Leite, R. H. de L., Silva Júnior, M. Q. da, Santos, F. K. G. dos, & Aroucha, E. M. M. (2019). Influence of composition on mechanical properties of cassava starch, sisal fiber and carnauba wax biocomposites. *Materials Research*, 22, 8877.
 34. Kawijia, K., Atmaka, W., & Lestariana, S. (2017). Study of characteristics whole cassava starch based edible film with citric acid cross-linking modification. *Jurnal Teknologi Pertanian*, 18(2), 143–152.
 35. Sholichah, E., Purwono, B., & Nugroho, P. (2017). Improving properties of arrowroot starch (*Maranta arundinacea*)/PVA blend films by using citric acid as cross-linking agent. *IOP Conference Series: Earth and Environmental Science*, 101, 012018.
 36. Chen, W. C., Nor, S., Ghazali, S. K., Dayangku Intan Munthoub, Alias, H., Mohamad, Z., & Majid, R. A. (2021). The effects of citric acid on thermal and mechanical properties of crosslinked starch film. *Chemical Engineering Transactions*, 83, 199–204.
 37. Guo, X., & Wu, Y. (2017). Characterizing Molecular structure of water adsorbed by cellulose nanofiber film using in situ micro-FTIR spectroscopy. *Journal of Wood Chemistry and Technology*, 37(5), 383–392.
 38. Hofstetter, K., Hinterstoisser, B., & Salmén, L. (2006). Moisture uptake in native cellulose – the roles of different hydrogen bonds: a dynamic FT-IR study using Deuterium exchange. *Cellulose*, 13(2), 131–145.
 39. Kalutskaya, E. P., & Gusev, S. S. (1980). An infrared spectroscopic investigation of the hydration of cellulose. *Polymer Science U.S.S.R.*, 22(3), 550–556.
 40. Saberi, B., Vuong, Q. V., Chockchaisawasdee, S., Golding, J. B., Scarlett, C. J., & Stathopoulos, C. E. (2016). Mechanical and physical properties of pea starch edible films in the presence of glycerol. *Journal of Food Processing and Preservation*, 40(6), 1339–1351.
 41. Wang, L., Kan, J., Tang, L., & Abidin, S. Z. (2025). The effects of glycerol addition on the

- physicochemical, structural and mechanical properties of salt-gelatinized rice starch-based film. *LWT*, 218, 117427.
42. Kowalczyk, D., Kazimierczak, W., Zięba, E., Lis, M., & Wawrzkiwicz, M. (2024). Structural and physicochemical properties of glycerol-plasticized edible films made from pea protein-based emulsions containing increasing concentrations of candelilla wax or oleic acid. *Molecules*, 29(24), 5998.
 43. Berube, M.-A., Schorr, D., Ball, R. J., Landry, V., & Blanchet, P. (2017). Determination of in situ esterification parameters of citric acid-glycerol based polymers for wood impregnation. *Journal of Polymers and the Environment*, 26(3), 970–979.
 44. Diniz, C. S., Souza, P. P. de, & Patricio, P. S. O. (2025). Viability of chemical modification of thermoplastic starch with citric acid through reactive extrusion. *Materials Research*, 28, 595.
 45. Santos-Iparraguirre, M., Chiralt, A., Martin-Esparza, M. E., & González-Martínez, C. (2026). Low-starch potato peel for the development of starch-based composites obtained by thermocompression moulding. *Sustainable Food Technology*, 4(2), 2171–2186.
 46. Nurazzi, N. M., Asyraf, M. R. M., Rayung, M., Norraahim, M. N. F., Shazleen, S. S., Rani, M. S. A., Shafi, A. R., Aisyah, H. A., Radzi, M. H. M., Sabaruddin, F. A., Ilyas, R. A., Zainudin, E. S., & Abdan, K. (2021). Thermogravimetric analysis properties of cellulosic natural fiber polymer composites: A review on influence of chemical treatments. *Polymers*, 13(16), 2710.
 47. Gutiérrez, P., Gervacio, A., & Valle, V. (2026). Agro-industrial lignocellulosic microparticles as functional reinforcements in sustainable poly(vinyl alcohol)/chitosan biofilms. *Materials & Design*, 115881.
 48. Wei, L., McDonald, A. G., & Freitag, C. (2022). Starch-based biodegradable materials: Challenges and opportunities. *Polymers*, 14(8), 1603.
 49. Anglès, M., & Dufresne, A. (2000). Plasticized starch/tunicin whiskers nanocomposites. 1. Structural analysis. *Macromolecules*, 33(22), 8344–8353.
 50. Dufresne, A., & Castaño, J. (2016). Polysaccharide nanomaterial reinforced starch nanocomposites: A review. *Starch – Stärke*, 69(1–2), 307.
 51. Mathew, A., & Dufresne, A. (2002). Morphological investigation of nanocomposites from sorbitol plasticized starch and tunicin whiskers. *Biomacromolecules*, 3(3), 609–617.
 52. Maiti, S., Ray, D., Mitra, D., Sengupta, S., & Kar, T. (2011). Structural changes of starch/polyvinyl alcohol biocomposite films reinforced with microcrystalline cellulose due to biodegradation in simulated aerobic compost environment. *Journal of Applied Polymer Science*, 122(4), 2503–2511.
 53. Bidari, R., Abdillah, A., Ponce, R., & Charles, A. (2023). Characterization of biodegradable films made from taro peel (*Colocasia esculenta*) starch. *Polymers*, 15(2), 338.
 54. Ostadi, H., Hakimabadi, S., Nabavi, F., Vossoughi, M., & Alemzadeh, I. (2020). Enzymatic and soil burial degradation of corn starch/glycerol/sodium montmorillonite nano composites. *Polymers from Renewable Resources*, 11(1–2), 15–29.
 55. Yoon, H. S., Lee, J., & Park, K. (2013). Cross-linked potato starch-based films using citric acid as crosslinker and plasticizer. *Journal of Agricultural and Food Chemistry*, 61(12), 2960–2970.
 56. Namphonsane, N., Chai, S. S. P. J., & Charoen, P. K. K. (2023). Toward a circular bioeconomy: Citric acid-modified thermoplastic starch blends with improved moisture resistance. *Membranes*, 13(5), 458.